Carbohydrate Research, 121 (1983) 13–30
Elsevier Science Publishers B.V., Amsterdam – Printed in The Netherlands

RHEOLOGY AND MICROSTRUCTURE OF DISPERSIONS AND SOLUTIONS OF THE MICROBIAL POLYSACCHARIDE FROM *Xanthomonas campestris* (XANTHAN GUM)

VICTOR J. MORRIS, DAVID FRANKLIN, AND KENNETH I'ANSON
ARC Food Research Institute, Colney Lane, Norwich NR4 7UA (Great Bruain)
(Received December 13th, 1982; accepted for publication, March 3rd, 1983)

ABSTRACT

A combination of various techniques, including rheology, light-scattering, photon correlation spectroscopy, optical rotation, and electric birefringence, has been applied to xanthan solutions and dispersions. The properties of the dispersions are consistent with a weak, gel-like network of highly associated xanthan molecules. Centrifugation or heat treatment disrupts this structure, resulting in a solution of individual molecules plus aggregates or "microgels". Filtration of these samples, or heat treatment of dispersions in the presence of urea, removes most of the microgels, leaving true solutions. In the true solutions, the molecules are rod-like with a molecular weight of 1.1×10^6 and rod lengths of 0.2–2 μm. In solutions of low ionic strength, the molecules show an order–disorder transition. However, the high-temperature-disordered form remains extended and rod-like. The helical backbone structure is apparently retained on cooling, even in the presence of urea. Minor structural changes involving disorganisation of the side chains could account for the ability of urea to inhibit aggregation. The microgels appear to consist of a side-by-side association of up to 47 individual molecules.

INTRODUCTION

The pathogenic micro-organism *Xanthomonas campestris* was first discovered in the vascular system of the Rutabaga plant. Infected areas were coated with a sticky slime caused by an exuded polysaccharide now known as xanthan gum. Aqueous dispersions of the polysaccharide are characterised by high viscosities at low rates of shear and by marked shear-thinning behaviour. These properties, together with the retention of a high viscosity at high ionic strength and over a wide range of temperatures, have led to wide and diverse industrial applications and to commercial cultivation of the micro-organism for polysaccharide production[1,2].

Structural studies suggest that the polymer repeat-unit may be a pentasaccharide[3,4]. The backbone consists of a chain of (1→4)-linked β-D-glucosyl residues with a trisaccharide side-chain linked at O-3 of alternate glucosyl residues. The

0008-6215/83/$ 03.00

composition of the side chain is *O*-β-D-mannopyranosyl-(1→4)-*O*-(α-D-glucopyranosyluronic acid)-(1→2)-*O*-(6-*O*-acetyl-β-D-mannopyranosyl). The terminal D-mannosyl groups may contain 4,6-acetal-linked pyruvic acid. Pyruvate substitution is variable, and dependent on the bacterial strain and the fermentation conditions[5,6].

X-Ray fibre-diffraction studies suggest[7,8] that the polymer may adopt a five-fold helical structure with an axial repeat-length of 4.7 nm. The data have been taken to suggest that the side chains bind non-covalently to the polymer backbone and stabilise the helical structure. Xanthan is difficult to crystallise and the resulting, poorly resolved X-ray pictures make it impossible to discriminate between single and multistranded helical structures. Multistranded models for xanthan have been proposed[9].

Rheological studies have been made on aqueous dispersions of xanthan prepared at room temperature[10–12]. The high viscosity and marked shear-thinning behaviour have been attributed to a rod-like character for the molecule. Current debate centres around the ratio of the persistence length of the molecule to the contour length as determined from measurements of molecular weight[12]. Structural studies of aqueous dispersions yield high and variable molecular weights[12,13]; values as high as 50×10^6 have been reported. Sedimentation studies have been taken[12] to suggest that these dispersions contain aggregates or microgels of high molecular weight. Similar conclusions have been drawn from filtration studies carried out in connection with the use of xanthan in enhanced oil-recovery applications[14,15]. These results have been taken to suggest that dispersions contain incompletely solvated polymer and are not true solutions. Hence, interpretations of rheological properties, measured on dispersions of xanthan, in terms of molecular size and shape should be treated with caution.

Centrifugation and ultrafiltration of dispersions or heat treatment (90°, 3 h) in the presence of 4M urea results in what have been termed true solutions of xanthan[13,16]. Determinations of molecular weight suggest that they are low and reasonably constant ($1–3 \times 10^6$). A variety of physical techniques has been applied to xanthan solutions in order to determine the conformation of the molecule. Studies using optical rotation, circular dichroism, and n.m.r. spectroscopy have been taken to suggest that xanthan exists in a helical form in solution, and it is believed that the helix is stabilised by binding of the side chains to the backbone[17,18]. Whether xanthan exists as a single or multistranded helix remains a topic of current debate[19,20]. Evidence for an order–disorder transition on heating solutions of low ionic strength comes from optical rotation studies[17,18,20]. The transition temperature increases with increasing ionic strength[17,18,20]. This stabilisation of the ordered (helical) structure has been used to explain the insensitivity of solution viscosity to ionic strength and temperature at moderately high ionic strengths. Further evidence favouring a highly extended, rod-like structure comes from light-scattering studies of solutions of the native polymers and a range of fractions of low molecular weight prepared by sonication[19], and from the appearance of quiescent birefringence[21] and cholesteric liquid-crystal behaviour[22] above certain concentrations

of polymer. Evidence for a rod-like structure following heat treatment in 4M urea has been obtained from studies of transient electric birefringence[23].

Thus, most rheological studies have been made on dispersions where there is evidence for polymer association. Most structural studies have been made on solutions in which aggregation has been largely eliminated. Studies of aqueous solutions show evidence for a time-dependent aggregation of xanthan molecules[13,24,25]. Present evidence suggests that such aggregation is inhibited by the presence of urea[13,26]. In the present studies, attempts have been made to investigate the rheology and micro-structure of xanthan for dispersions and solutions in water and in urea. Structural studies include the use of optical rotation, conventional light-scattering, photon correlation spectroscopy, and transient electric birefringence. In particular, we have concentrated on observing the conformation and interaction of xanthan molecules under conditions which markedly affect the rheological properties.

MATERIALS AND METHODS

Sample preparation. — Samples of xanthan gum (Sigma) were dispersed in deionised distilled-water and centrifuged to remove cell debris. Clarification was checked by phase-contrast and electron microscopy. Typically, a 0.1% solution was centrifuged at 76,000*g* for 1–3 h. This clarified solution was ion-exchanged into the sodium form by using Dowex 50X-W8 (Na^+) resin, and then freeze-dried.

Aqueous dispersions were prepared by adding the clarified powder to ~75% of the required volume of deionised distilled-water and stirring overnight at room temperature. Samples were then diluted to the required volume and stirred until homogeneous, as judged visually. Dispersions in urea were prepared in a similar manner with the required quantity of urea added as powder. All solutions contained 0.02% of sodium azide as a preservative. Concentration ranges were prepared by dilution of these stock dispersions with the correct solvent. Stock dispersions were stored at 4°.

Heat treatment of dispersions in water or urea involved keeping the samples at 90° for 3 h and then cooling to room temperature. Solvent was added to correct for solvent losses on heating.

Further clarification of solutions or dispersions for optical studies involved centrifugation and/or ultrafiltration. Centrifugation was carried out at 100,000*g* for 1 h. In the case of dispersions, deposition of gel-like material occurred. Typically, for a 0.1% dispersion, the gel-like deposit amounted to ~15% of the total mass of the polymer. No deposition of gel-like material was observed for heat-treated dispersions. Filtration involved the use of 0.22-μm Millipore filters. Dispersions proved impractical to filter. The passage of sample was extremely slow and excessive loss of polymer occurred. The supernatant obtained after centrifugation could be filtered with difficulty, as could heat-treated aqueous dispersions. Typically, for a 0.1% solution, the polymer loss was up to ~5% of the total polymer mass. Heat-

treated samples in urea were comparatively easy to filter, and there were no detectable losses of polymer.

Rheology. — A Deer rheometer (Rheometer Marketing Ltd., Armley Road, Leeds, Great Britain) was used, with concentric cylindrical geometry. The radii of the inner rotor and the outer container were 1.8 and 2 cm, respectively. The rotor length was 6.5 cm. Measurements were made using an end-gap setting of 76 μm. Calculation of shear stress, shear rate, shear strain, and end-effect corrections were made by standard procedures[27]. Typically, shear stresses in the range 10^{-2}–2.5 $N.m^{-2}$ were applied in the form of a ramp lasting 5–20 s, and then held constant. Relaxation studies were made following "instantaneous" release of the applied shear-stress. The apparatus was thermostatted, and measurements were made at 24°.

Photon correlation spectroscopy (p.c.s.). — P.c.s. measurements were made by homodyne detection[28] using a Malvern 4300 spectrometer (Precision Devices Ltd., Malvern, Great Britain). The light source was a 15-mW helium–neon laser operating at a wavelength of 0.633 μm. Scattered light was measured over the angular range 30–150°. The scattering was monitored by using an EMI 9863KB/100 photon counting-tube. Analysis was performed with a K7023 Malvern autocorrelator interfaced to a PET 32K microcomputer. Single, clipped autocorrelation was employed[28]. The background was calculated from the unclipped count-rate, the clipped count-rate, and the total number of samples. Results were expressed in terms of the correlation function[28] $g^2(t)$ written in the form $[g^2(t) - 1]$ and normalised with respect to its value at zero elapsed time $[g^2(0) - 1]$.

The apparatus was thermostatted, and measurements were made over the range 24–95°. Dispersions were clarified by centrifugation at 5000*g* for 1 h. Heat-treated dispersions were filtered through 0.22-μm filters.

Light-scattering. — Conventional light-scattering studies were made with the Malvern 4300 Spectrometer system. The incident light was vertically polarised, and a parallel incident beam was used instead of the focused beam employed for p.c.s. studies. Glass scintillation-vials (diameter, 2.5 cm) were used as scattering cells. The alignment of the instrument was checked by measuring the angular dependence of light scattered by filtered samples of benzene. Measurements were made relative to benzene. The Rayleigh ratio ($R_{90°}$) for benzene was estimated to be 8.8 $\times 10^{-8} m^{-1}$ on the basis of values given at different wavelengths[29]. The Cabannes factor[30] was used to correct for depolarisation effects for the benzene samples, assuming a value of 2.6. The depolarisation ratio for xanthan samples was assumed to be negligible. Scattered intensities were measured by using the autocorrelator in the signal-averaging mode and counting for 0.9 s. The scattered intensity at each angle was monitored for periods of time up to 48 s. Measurements were made over the angular range 30–120°. Values of dn/dc for samples in water[16] and 4M urea[13] were taken as 0.144 and 0.135, respectively. The absolute calibration of the instrument was checked by determining the molecular weight of bovine serum albumin in 0.01M NaCl (pH 6.8) at 24°. A value of (64 ±6) $\times 10^3$ was obtained, which com-

pares favourably with values reported in the literature[31]. The same sample gave a value of (5.6 ±0.1) × 10^{-11} $m^2.s^{-1}$ for the translational diffusion coefficient from p.c.s. studies, which was also in good agreement with the reported value[32] of 5.76 × 10^{-11} $m^2.s^{-1}$.

Transient electric birefringence (t.e.b.). — The t.e.b. equipment was constructed at the Food Research Institute to a standard design[33]. The apparatus has been described in detail[23].

Optical rotation. — These measurements were kindly made by Dr. A. J. Clarke-Sturman (Shell Research Centre, Sittingbourne, Kent) with a Perkin–Elmer 241 polarimeter and a Haake temperature-programmed water-bath. Traces were obtained at 0.365 μm, and several heating and cooling cycles were measured.

RESULTS

Rheology. — Fig. 1 illustrates the effect of various treatments on the viscosity of 0.11% xanthan dispersions. Dispersions in water and 4M urea show similar behaviour and both display marked shear-thinning behaviour. The present results are compatible with data[10–12] for aqueous dispersions of xanthan. At low-shear stress, the samples show evidence for instantaneous and retarded elastic responses and flow (Fig. 2). The elastic response decreased with increasing shear-rate, but recovered on standing.

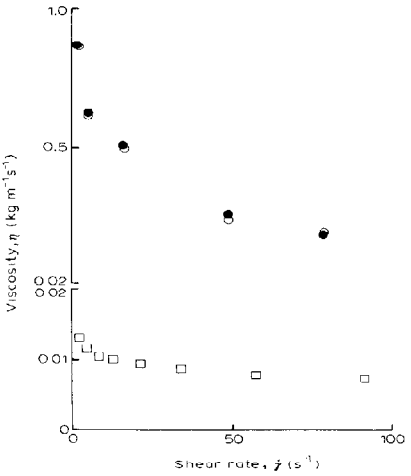

Fig. 1. Plots of viscosity *versus* shear rate for various preparations of xanthan: xanthan concentration, 0.11%; ●, aqueous dispersion; ○, dispersion in 4M urea; □, dispersion in 4M urea following heat treatment at 90° for 3 h.

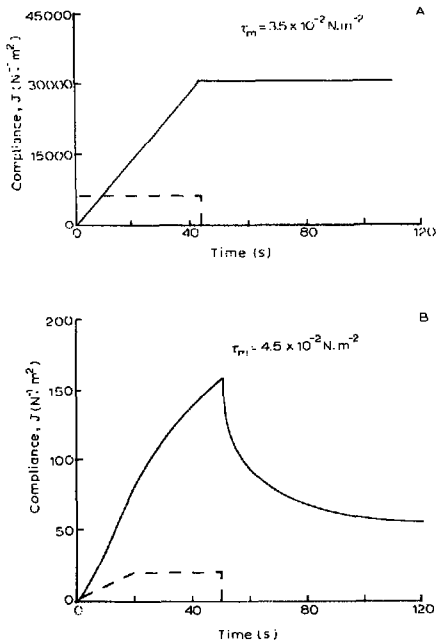

Fig. 2. Representative plots of compliance (J) against time (t) for xanthan (0.11%); the applied stress profile is indicated by ---, and the maximum stress (τ_m) values are recorded: A, heat-treated sample in 4M urea with $\tau_m = 3.5 \times 10^{-2}$N.m^{-2}; B, aqueous dispersion with $\tau_m = 4.5 \times 10^{-2}$N.m^{-2}.

Various treatments markedly affected the shear-rate viscosity and the shear-thinning behaviour. The treatments that yielded samples with the lowest viscosities and smallest shear-thinning behaviour were (*a*) heat treatment in 4M urea, and (*b*) ultracentrifugation of dispersions (Fig. 1). These "solutions" showed no evidence of elastic responses (Fig. 2) and no significant increase in viscosity on standing.

The viscosity of heat-treated samples in water showed behaviour intermediate between that of the "dispersions" and the "solutions". In all cases measured, the viscosities for aqueous dispersions were higher than those for dispersions in urea following similar treatments (Fig. 1).

Optical rotation. — Studies were made on aqueous dispersions of xanthan prepared at room temperature and on heat-treated dispersions in water and 4M urea. In all cases, heating and cooling curves were reversible with little hysteresis. Data for an aqueous 0.1% dispersion are shown in Fig. 3. At room temperature, the large negative rotation is comparable with data for samples of comparable

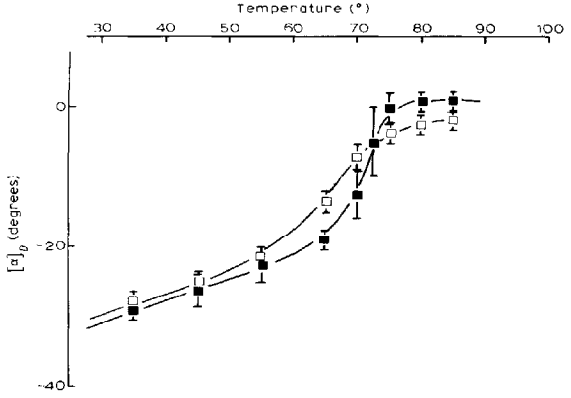

Fig. 3. Optical rotation *versus* temperature plots obtained for 0.1% solutions of xanthan heat-treated in aqueous solution (—■—) and in 4M urea (—□—). The error bars reflect the variation in optical rotation values observed on successive heating and cooling cycles.

sodium molarity[17,18,20]. Data obtained for heat-treated xanthan solutions in 4M urea are also shown in Fig. 3. The curves are similar to those obtained for aqueous dispersions. The rotation values at room temperature are similar, but the transition temperature range is broadened. These results differ both qualitatively and quantitatively with data reported by Southwick *et al.*[34–36], but accord with results reported by Frangou *et al.*[26].

Photon correlation spectroscopy (p.c.s.). — Fig. 4 shows comparative studies of the normalised correlation functions $\{[g^{(2)}(t) - 1]/[g^{(2)}(o) - 1]\}$ obtained for 0.1% xanthan samples prepared by various methods. Aqueous dispersions were characterised by correlation functions exhibiting slowly decaying tails. Centrifugation and filtration, or heat treatment of dispersions in 4M urea, yield correlation functions that are experimentally indistinguishable (Fig. 4). These functions show no evidence of slowly decaying tails, and drop to zero over periods of elapsed time of the order of 30 ms. Heat treatment of aqueous dispersions yielded intermediate behaviour (Fig. 4). On filtration of the dispersions, the curves approximated to those obtained after heat treatment in 4M urea. Fig. 5 shows the effect of heat treatment on samples as a function of urea concentration in the range 2–8M urea.

Subsequent studies were concentrated on solutions of xanthan prepared either by centrifugation and filtration, or by heat treatment and filtration, of aqueous dispersions. For a monodisperse system of point-dipole scatterers, the normalised correlation function should be a single exponential decay[28] characterised by a half-width $\Gamma = 2D_T K^2$, where K is the modulus of the wavevector given by $K = (4\pi n_0/\lambda)\sin(\theta/2)$, n_0 is the refractive index of the solvent, λ is the vacuum

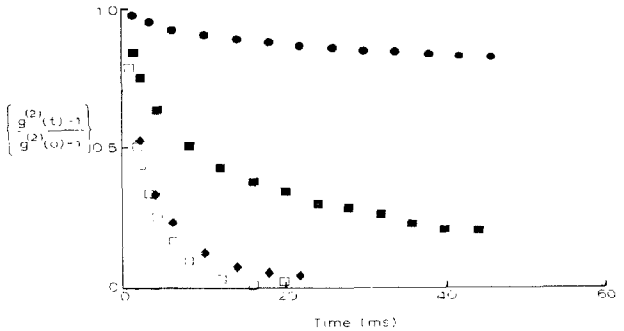

Fig. 4. Normalised autocorrelation functions $\{[g^{(2)}(t) - 1]/[g^{(2)}(o) - 1]\}$ plotted against elapsed time (t) for 0.1% xanthan preparations at 22°: ●, aqueous dispersion; ■, heat-treated aqueous dispersion; ◆, centrifuged and filtered aqueous sample; □, heat-treated sample in 4M urea. Scattering angle, 40°.

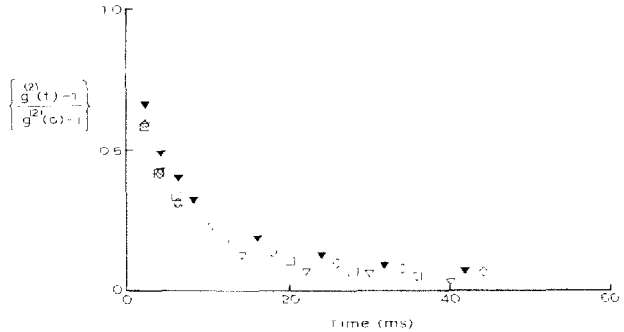

Fig. 5. Normalised autocorrelation functions $\{[g^{(2)}(t) - 1]/[g^{(2)}(o) - 1]\}$ plotted against elapsed time (t) for heat-treated 0.1% xanthan samples at various concentrations of urea: ○, 2M; □, 4M; ▽, 6M; and ▼, 8M urea. Scattering angle, 40°. Temperature, 22°.

wavelength of the incident light, and θ is the scattering angle. For polydisperse systems[28], the initial slope of a semi-logarithmic plot of $\{[g^{(2)}(t) - 1]/[g^{(2)}(o) - 1]\}$ against elapsed time t yields a z-average value of the translational diffusion coefficient $\langle D_T \rangle_z$; for grossly polydisperse systems, this average value $\langle D_T \rangle_z$ will be dependent on the sample time and it is necessary to extrapolate the measured values to zero sample-time.

Values of Γ approximated to constant values at sample times below 15 μs. The semilog plots of the normalised correlation function showed marked curvature. Variations in the measured Γ values at large sample-times were traced to fluctuations in the measured background value of $\{[g^{(2)}(t) - 1]/[g^{(2)}(o) - 1]\}$; observed at large times.

TABLE I

PARAMETERS[a] MEASURED FOR XANTHAN SAMPLES FOLLOWING HEAT TREATMENT OF AQUEOUS OR 4M UREA DISPERSIONS

	Heat-treated aqueous sample		*Heat-treated 4M urea sample*	
Property	*Experimental*	*Calculated*	*Experimental*	*Calculated*
$\langle M \rangle_w$	$(47 \pm 5) \times 10^{6b}$	—	$(1.1 \pm 0.1) \times 10^{6b}$	—
$\langle R_g^2 \rangle_z^{1/2}$ (μm)	$(0.26 \pm 0.05)^b$	0.36	$(0.24 \pm 0.04)^b$	0.28
$\langle D_T \rangle_z$ ($m^2.s^{-1}$)	$(2.5 \pm 0.6) \times 10^{-12c}$	2.3×10^{-12}	$(2.7 \pm 0.6) \times 10^{-12c}$	2.3×10^{-12}
σ	0.7 ± 0.1	—	0.6 ± 0.1	—
m (μm)	(0.60 ± 0.01)	—	(0.58 ± 0.01)	—

[a]Theoretical parameters calculated on the basis of the length distributions shown in Fig. 10 are also given. In these calculations, the axial ratio has been approximated by the mean value $\bar{p} = (m/d)\exp(\sigma^2/2)$. [b]Filtration through 0.45-μm filters. [c]Filtration through 0.22-μm filters.

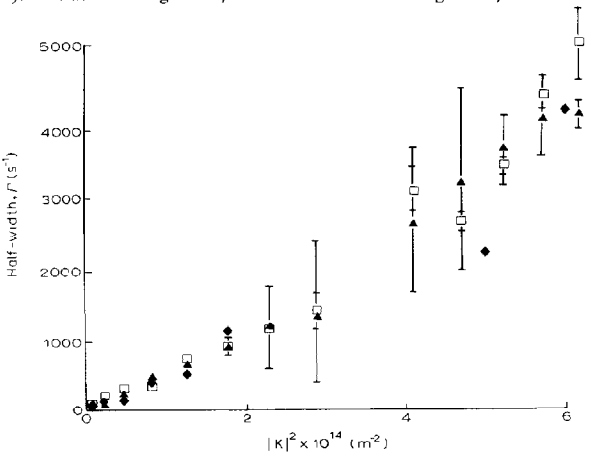

Fig. 6. Plot of the half-width ($\Gamma = 2\ D_T K^2$) against the square of the modulus of the scattering vector (K) for 0.1% xanthan samples at 22°: □, heat-treated sample in 4M urea; ▲, centrifuged aqueous dispersion; ◆, centrifuged and filtered aqueous dispersion. The error bars indicate the spread in the data obtained after a series of experiments.

Fig. 6 shows plots of Γ as a function of K^2 for aqueous dispersions after centrifugation and filtration, and for heat-treated samples in 4M urea. The dependence of Γ on K^2 was linear over the angular range $\theta < 60°$, and the data for the two samples were similar. The slope of the plot yielded values of $\langle D_T \rangle_z$ as given in Table I. Above 60°, small departures from linear behaviour were observed. The data shown in Fig. 6 were measured at a polymer concentration of 0.1%. Studies of the dependence of $\langle D_T \rangle_z$ on polymer concentration and on urea concentration showed no significant variations.

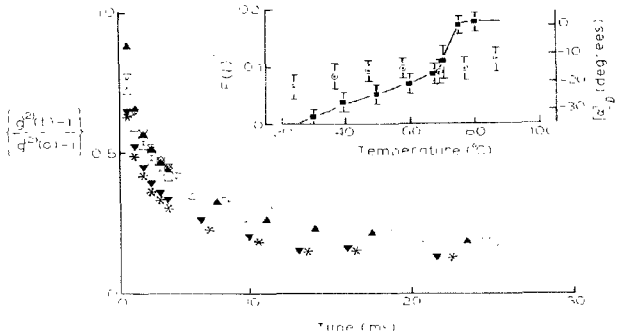

Fig. 7. Plots of the normalised autocorrelation functions $\{[g^{(2)}(t) - 1]/[g^{(2)}(o) - 1]\}$ as a function of temperature: ▲, 24°; ▽, 37°; △, 47°; ○, 59°; ▼, 69°; ✱, 77°. Xanthan concentration, 0.1%; scattering angle, 40°. The insert shows a comparison of the temperature dependence of the optical rotation (■) and the parameter $F(l)^{-1} = kT/(3\pi\eta D_T)$ as calculated from the initial slopes of the correlation functions (○).

Fig. 7 shows an attempt to observe the effect of temperature on polymer motion in a xanthan solution of low ionic strength. The sample employed was a centrifuged, aqueous dispersion. Samples were heated to each required temperature and allowed to equilibrate for 10 min. D_T may be written in the form[28] $(kT/3\pi\eta l)F(l)$, where η is the viscosity of the suspending medium, k is Boltzmann's constant, l is the rod length, d is the rod diameter, T is the absolute temperaure, and $F(l)$ is a function dependent on the size and shape of the polymer. For a rod-shaped particle[37], $F(l) = \{\ln(2l/d) - 0.11\}$. The insert in Fig. 7 shows both the variation in $F(l)^{-1}$ and the variation in optical rotation obtained on heating the sample.

Light-scattering. — Conventional light-scattering studies were made on heat-treated dispersions in water and in 4M urea. The scattered intensity for heat-treated aqueous samples was sensitive to the filtration process. Samples were filtered once through 0.45-μm Millipore filters. Heat-treated samples in 4M urea were observed by the same method. Scattering measurements were made in the concentration range 0.2–0.025%, and data were analysed by the Zimm-plot method. Values of the weight-average molecular weight $\langle M\rangle_w$ and the square root of the z-average square of the radius of gyration $\langle R_z^2\rangle_z^{1/2}$ are given in Table I.

Transient electric birefringence (t.e.b.). — T.e.b. studies of heat-treated xanthan solutions in 4M urea have been described in detail[23]. Here, we are concerned with comparative studies of heat-treated aqueous and 4M urea dispersions of xanthan. The sign of the birefringence was positive for both types of solution. At low electric-field amplitudes, both samples obeyed the Kerr law[43], and the birefringence saturated at sufficiently large electric-field amplitudes. Fig. 8 shows plots of the saturation birefringence (Δn_s) for the two types of solution as a function of polymer concentration. In both instances, Δn_s varied linearly with polymer concen-

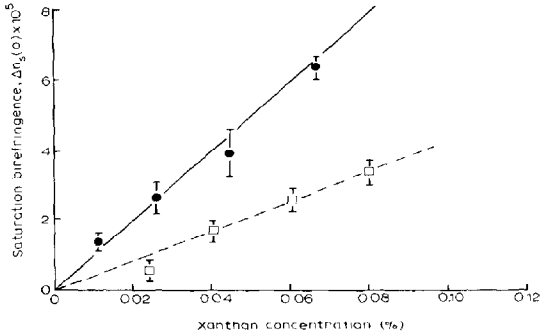

Fig. 8. Plots of the saturation birefringence Δn_s against concentration of polymer for aqueous (●) and heat-treated in 4M urea (□) solutions.

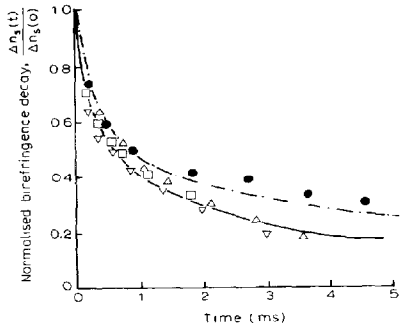

Fig. 9. Plots of the normalised birefringence decay-curves for aqueous and 4M urea solutions. The decay curves were measured using electric field amplitudes sufficient to induce full orientation at t = 0: ●, 0.066% aqueous solution; □, 0.08%, △, 0.06%; and ▽, 0.04% solutions in 4M urea. The lines represent theoretical decay-curves calculated assuming a log-normal distribution: — · —, aqueous solution, $\sigma = 0.7$, m = 0.6 μm; ——, 4 M urea solution, $\sigma = 0.6$, m = 0.58 μm).

tration. At a given concentration, Δn_s was larger for aqueous solutions than for solutions in 4M urea. Fig. 9 shows normalised decay-curves from full orientation for heat-treated samples in water and 4M urea. In both cases, the relaxation spectra were of a similar order of magnitude. No significant dependence on concentration was observed. Semi-logarithmic plots of the decay curves were curved, indicating a distribution of relaxation times.

DISCUSSION

The experimental data collected here suggest that the rheology and microstructure of xanthan preparations are sensitive to the methods of preparation. At low ionic strength, two extreme modes of behaviour were observed. Following Dintzis *et al.*[13], room-temperature preparations are referred to as *dispersions*. Samples prepared by centrifugation and/or ultrafiltration of dispersions are termed true *solutions*.

In the present studies, it was noted that dispersions are characterised by high viscosities and marked shear-thinning behaviour (Fig. 1). In 0.1% preparations at low shear-stresses, evidence for elastic responses was observed (Fig. 2). P.c.s. studies of molecular motion yielded autocorrelation functions characterised by extremely long relaxation-times (Fig. 4). These relaxation times are too long to be attributed to free macromolecular diffusion.

Solutions of xanthan in both water and urea are characterised by the loss of detectable elastic-responses (Fig. 2), lower viscosities, and weak shear-thinning behaviour (Fig. 1). Studies of polymer motion in these systems by p.c.s. (Figs. 4 and 5) and t.e.b. methods (Fig. 9) are characterised by comparatively fast relaxation-processes compatible with unhindered diffusional motion.

The above changes were irreversible. The true solutions showed no significant increase in viscosity over a period of several weeks. The minor increases in viscosity observed for heat-treated or centrifuged aqueous dispersions were inhibited by the presence of urea. The irreversible changes accompanying thermal treatment of xanthan dispersions are not accompanied by irreversible changes in optical rotation. The room-temperature values of optical rotation for heat-treated dispersions in water and 4M urea are compatible with reported values for the ordered (helical) structure. This suggests that irreversible changes illustrated in Figs. 1, 2, and 4 resulted from a dissociation of an ordered form of the polymer rather than a denaturation of the ordered structure. This accords with the data of Frangou *et al.*[20], who also showed that removal of urea from a heat-treated sample by dialysis resulted in re-aggregation of polymers and significant increases in viscosity.

These results support the suggestion that the pseudoplastic behaviour of xanthan dispersions is due to the formation of a weak, tenuous, gel-like network[18]. Disruption of this network by centrifugation or thermal treatment would lead to a loss of elastic behaviour and a decrease in viscosity. However, the difficulties experienced in filtering such solutions suggest that large molecular aggregates may still be present. The existence of such aggregates or "microgels" has been proposed from filtration and porosity studies[14,15]. The data in Table I support this suggestion. Samples heat-treated in urea were easier to filter than heat-treated aqueous samples and their viscosities did not increase with time on standing. The molecular weight measured for heat-treated samples in 4M urea is markedly lower than that obtained for heat-treated aqueous samples. The values shown in Table I are typical of those reported in the literature[13].

Studies of solutions have been used to investigate the size and shape of the individual macromolecules, and the effects of heating and urea on solution properties. The optical rotation data obtained for heat-treated aqueous solutions are consistent with data reported elsewhere. It has been suggested that the optical rotation data are dominated by the relative conformations of the backbone sugars[17]. The decrease in optical rotation observed on heating solutions of low ionic strength has been attributed to a transition from an ordered helical structure into a disordered coil. Reported n.m.r. and c.d. data have been taken to suggest that the side chains are disordered at high temperatures. At low temperatures, these side chains are believed to stabilise the helical structure by binding non-covalently to the backbone[17]. It has been proposed that the rheological changes observed on heat treatment in 4M urea are due to an inhibition of hydrogen bonding by the urea, resulting in a preservation of the disordered form on cooling[34–36]. The optical rotation data reported here and elsewhere[26] clearly afford evidence for a reversible order–disorder transition (Fig. 3). Further, the rotation values at room temperature are the same for heat-treated solutions in water or 4M urea. Thus, if the optical rotation is dominated by the conformation of the backbone, the helical structure is re-formed on cooling in urea.

T.e.b. studies have been made on xanthan solutions in water and in 4M urea at room temperature. The normalised decay-curves shown in Fig. 9 suggest that the relaxation behaviour is similar for both solutions. As discussed elsewhere[23,38], the positive birefringence and the magnitudes of these relaxation times are characteristic of orientational polarisation[39] and suggest an extended rod-like structure. Further, the insensitivity of the relaxation behaviour to polymer concentration suggests independent, unhindered, rotational motion. To fully characterise our solutions in terms of molecular size and shape, it would be necessary to evaluate the persistence length (P) and the distribution of contour lengths (L). In principle, for a single relaxing-species, a value of P may be found from electro-optic data if L is known[40]. Determination of L requires knowledge of the molecular weight and the mass per unit length. The latter is a matter of debate[9,19,20]. This, coupled with the difficulty of discriminating between polydispersity and other modes of motion of the polymer, led us to use a simple estimate of particle size. Relaxation data were converted into particle sizes by treating the polymers as rigid rods and calculating an equivalent rod-length (l). The light-scattering data of Paradossi and Brant[19] provide evidence favouring a highly extended form of xanthan, and molecular weight determinations favour a skew distribution[41]. Previously[23], we evaluated the distribution of particle lengths $f(l)$ by comparing the average, rotary diffusion coefficients measured in the Kerr region and at full orientation. This procedure involves assumptions about the dependence of the electrical dipole moments on particle size[42]. To eliminate this assumption, $f(l)$ was evaluated by curve fitting an expression of the form

$$\frac{\Delta n_s(t)}{\Delta n_s(o)} = \{\int_0^\infty l f(l) \exp[-6D_R(l) \cdot t] dl\} / \{\int_0^\infty l f(l) dl\}.$$

where $f(l) = (2\pi)^{-1/2}(\sigma l)^{-1} \exp\{-\frac{1}{2}(\ln(l/m)/\sigma)^2\}$,
and $D_R(l) = (3kT/\pi\eta)l^{-3}(\ln(2\rho) - 0.8)$.

to the exponential decay-curve. Values of σ and m were adjusted to obtain the best fit to the experimental data. The equation employed for $D_R(l)$ is Burgers' equation[43], and that for $f(l)$ is the log-normal distribution[44]. In evaluating the integrals in the above equations, the axial ratio (ρ) was approximated by the mean value[42] $\bar{\rho} = (m/d)\exp(\sigma^2/2)$, where d is the rod diameter. The resulting distributions of equivalent rod-lengths are shown in Fig. 10, and are similar for aqueous and 4M urea solutions. From the parameters for the distribution functions shown in Fig. 10 (Table I), the estimated molecular weight of 1.1×10^6 gives a mass per unit-length of 1511 daltons/nm for the heat-treated sample in 4M urea. The calculated z-average values of $\langle R_g^2\rangle_z^{1/2}$ and $\langle D_T\rangle_z$ are given in Table I for solutions in water and 4M urea. The values calculated from the equivalent rod-length distributions (Fig. 10) agree with the values of $\langle D_T\rangle_z$ determined directly. However, the $\langle R_g^2\rangle_z^{1/2}$ values calculated from the distributions shown in Fig. 10 yield values slightly higher than the experimental values. This probably reflects flexibility of the rod-like structure as reported by Paradossi and Brant[19] from the dependence of $\langle R_g^2\rangle_z^{1/2}$ on molecular weight, and by Rinaudo and Milas[16] from the dependence of $\langle R_g^2\rangle_z^{1/2}$ on ionic strength. However, the data clearly indicate the highly extended rod-like character of xanthan molecules. Although the size and shape of the macromolecules are similar for aqueous and 4M urea solutions, the saturation birefringence data in Fig. 8 may reflect differences in molecular structure. In both cases, Δn_s varies linearly with concentration, implying independent molecules in the concentration range studied. However, Δn_s is larger for aqueous solutions than for solutions in 4M urea. If this difference results from a difference in molecular anisotropy, then, on the basis of the accepted interpretation of the optical rotation data, any such differences in molecular structure must surely result from disordering of the side chains. Possibly, urea inhibits binding of the side chains to the backbone; in turn, this could affect aggregation of the xanthan molecules. However, it is not immediately obvious why urea should inhibit binding of the side chains to the backbone but not inhibit formation of the helical structure itself. Perhaps irreversible chemical changes occur on heating with urea which lead to structural modifications. The formation of carbamates on heating starch with urea has been reported[45]. However, n.m.r. studies of xanthan samples heated in the presence of urea for periods up to 3 h show no evidence for amide formation or other detectable chemical modifications[26]. Further, the rheology of the untreated sample may be restored on removal of urea by dialysis, indicating no appreciable chain-cleavage[26].

P.c.s. studies of xanthan solutions should yield additional information on particle size and shape. Solutions prepared by centrifugation and ultrafiltration, or by heat-treatment and filtration, of dispersions in water or urea yielded correlation functions that were experimentally indistinguishable. Variations between samples were traced to variations in the experimental background values [$\{[g^{(2)}(t) -$

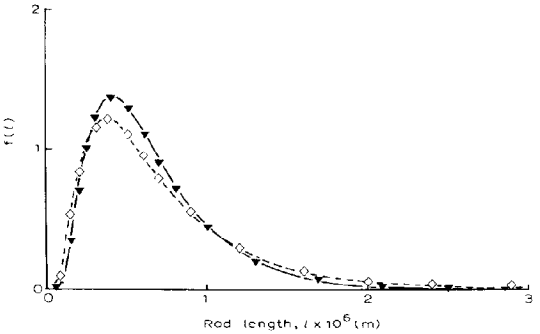

Fig. 10. Calculated length-distributions based on a log-normal distribution. These distributions provide the best fits to the experimental data shown in Fig. 9: —▼—, 4M urea solution; —◇—, aqueous solution.

$1]/[g^{(2)}(o) - 1]\}\rightarrow\infty]$. The z-average D_T values obtained after extrapolation to low sample-times are consistent with the size distributions shown in Fig. 10 (see Table I). However, attempts to assess particle shape from the angular dependence of Γ proved unconvincing. The dynamic form factor is given by[28]

$$S(Kl) = S_0(Kl)\exp(-D_TK^2t) + S_1(Kl)\exp[-(D_TK^2 + 6D_R)t] + \cdots,$$

where the terms $S_0(Kl)$, $S_1(Kl)$ are as defined in ref. 28. It is accepted[28] that the scattering becomes sensitive to particle shape and rotational motion as K increases. Hence, at $Kl \sim 5$, $S_1(Kl)$ becomes significantly large compared to $S_0(Kl)$, and the initial slope of the correlation function should depart from a K^2 dependence due to contributions from rotational diffusion. For a 0.6-μm rod, $\lambda = 0.633\ \mu$m, such a departure should occur at $\theta > 38°$. This was not observed experimentally (Fig. 6). However, it is possible to show that measurements of the dependence of Γ on K^2 do not provide an unequivocal test of particle shape. This is illustrated in Fig. 11. The terms $S_1(Kl)$ and $S_0(Kl)$ were calculated for a range of K and l values. Thus, in Fig. 11, the dependence of S_1, S_0, and R on particle size expected for a scattering angle of 40° is plotted. As expected, S_1 becomes significant with respect to S_0 for $l > 0.55\ \mu$m. However, for $l > 0.55\ \mu$m, the ratio R tends rapidly to unity, and hence Γ will be dominated by translational motion and remain K^2. A direct indication of this is seen in Fig. 12, where the inclusion of a rotational component into the calculation of $\{[g^{(2)}(t) - 1]/[g^{(2)}(o) - 1]\}$ has a negligible effect. Hence, studies of the angular dependence of Γ depend on the relative values of S_1 and S_0, and also on the relative values of D_T and D_R, and do not provide a simple guide to particle shape.

Attempts to curve-fit the complete correlation functions for xanthan solutions on the basis of the size distributions obtained in Fig. 10 were also unsuccess-

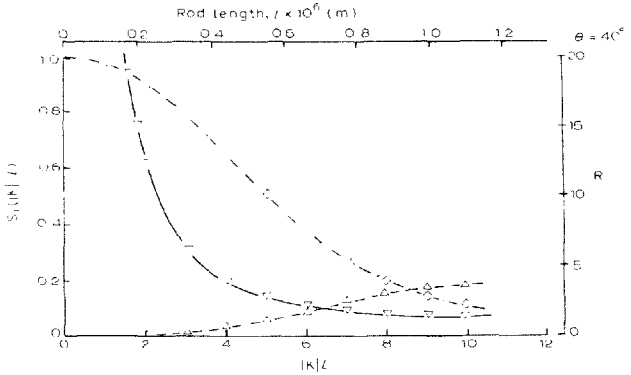

Fig. 11. Plots of the scattering functions S_1 (△), S_0 (◇), and the ratio $R = (D_T K^2 + 6D_R)/(D_1 K^2)$ (▽) as a function of Kl. The equivalent rod-lengths (l) for observations made at a scattering angle of 40° and a wavelength of 0.633 μm are also shown

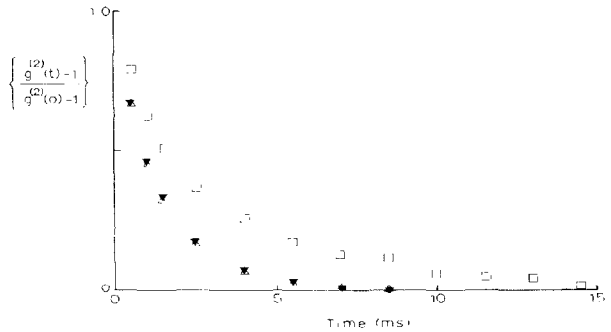

Fig. 12. Theoretical fits for the autocorrelation functions calculated on the basis of the length distributions shown in Fig. 10: □, 0.1% xanthan heat-treated in 4M urea, experimental data. △, theoretical fit based on $\sigma = 0.6$, $m = 0.58$ μm, and considering only translational diffusion. ▼, theoretical fit ($\sigma = 0.6$, $m = 0.58$ μm) taking into account both rotational and translational motion

ful. Even when polydispersity of both rotational and translational motion was taken into account, the theoretical curves only provide a good fit to the short-time behaviour of $\{[g^{(2)}(t) - 1]/[g^{(2)}(o) - 1]\}$ (Fig. 12). We believe that this results from incomplete removal of "microgels" or "aggregates". The presence of a small quantity of large molecular aggregates would give rise to a contribution to $\{[g^{(2)}(t) - 1]/[g^{(2)}(o) - 1]\}$ due to fluctuations in the number-density of these particles in the scattering volume.

The nature of the microgels is difficult to assess, because their properties will probably be sensitive to the detailed treatment of the dispersion prior to investigation. However, the data in Table I provide a guide to the association of the xanthan molecules. The data for heat-treated xanthan in 4M urea are taken to represent individual molecules. Thus, the aggregate observed in the heat-treated aqueous dispersion should contain ~47 molecules. The large change in molecular weight coupled with the small changes in $\langle R_g^2 \rangle_z^{1/2}$ suggest side–side association of the molecules, rather than the end–end association suggested in the models proposed by Holzwarth and Prestridge[9].

The data shown in Fig. 7 suggest that breakdown of xanthan association by heat treatment of dispersions of low ionic strength results from an order–disorder transition, as monitored by optical rotation. However, the p.c.s. studies show that this order–disorder transition is not accompanied by any major size or shape change of the entire molecule. If the helical structure is lost, the molecules still remain highly extended, possibly because of intramolecular steric or electrostatic interactions.

ACKNOWLEDGMENTS

The authors thank G. R. Chilvers, G. J. Brownsey, C. Turner, and S. G. Ring (FRI) for advice and assistance, and Dr. A. J. Clarke-Sturman (Shell Research Centre, Sittingbourne) for obtaining the optical rotation data. During the period of this work, C. Turner and D. Franklin were students in the Physics Department, Brunel University.

REFERENCES

1 T. R. Andrew, in P. A. Sandford and A. Laskin (Eds.), *Extracellular Microbial Polysaccharides, ACS Symp. Ser*, 45 (1977) 231–241.
2 E. L. Sandvik and J. M. Maerber in P. A. Sandford and A. Laskin (Eds.), *Extracellular Microbial Polysaccharides, ACS Symp. Ser*, 45 (1977) 242–264.
3 P.-E. Jansson, L. Kenne, and B. Lindberg, *Carbohydr. Res.*, 45 (1975) 275–282.
4 L. D Melton, L. Mindt, D. A. Rees, and G. R. Sanderson, *Carbohydr. Res.*, 46 (1976) 245–257.
5 M. C. Cadmus, S. P. Rogovin, K. A. Burton, J. E. Pittsley, C. A. Knutson, and A. Jeanes, *Can. J. Microbiol.*, 22 (1976) 942–948.
6 M. C. Cadmus, C. A. Knutson, A. A. Lagoda, J. E. Pittsley, and K. A. Burton, *Biotechnol. Bioeng.*, 20 (1978) 1003.
7 R. Moorhouse, M. D. Walkinshaw, and S. Arnott, in P. A. Sandford and A. Laskin (Eds.), *Extracellular Microbial Polysaccharides, ACS Symp. Ser.*, 45 (1977) 90–102.
8 K. Okuyama, S. Arnott, R. Moorhouse, M. D. Walkinshaw, E. D. T. Atkins, and C. H. Wolf-Ullish, in A. D. French and K. H. Gardener (Eds.), *Fiber Diffraction Methods, ACS Symp. Ser.*, 141 (1980) 411–427.
9 G. M. Holzwarth and F. G. Prestridge, *Science*, 197 (1977) 757–759.
10 P. J. Whitcomb, B. J. Ek, and C. W. Macosko, in P. A. Sandford and A. Laskin (Eds.), *Extracellular Microbial Polysaccharides. ACS Symp. Ser.*, 45 (1977) 160–173.
11 P. J. Whitcomb and C. W. Macosko, *J. Rheology*, 22 (1978) 493–505.
12 G. M. Holzwarth, in D. A. Brant (Ed.), *Solution Properties of Polysaccharides, ACS Symp Ser.*, 150 (1981) 15–23.

13 F. R. DINTZIS, G. E. BABCOCK, AND R. TOBIN, *Carbohydr. Res.*, 13 (1970) 257–267.
14 N. KOHLER AND G. CHAUVETEAU, SPE 7425 Technical Conference and Exhibition of the Society of Petroleum Engineers of AIME, Houston, Texas, U.S.A., Oct. 1–3 (1978).
15 G. CHAUVETEAU AND N. KOHLER, SPE 9295 Technical Conference and Exhibition of the Society of Petroleum Engineers of AIME, Dallas, Texas, U.S.A., Sept. 21–24 (1980).
16 M. RINAUDO AND M. MILAS, *Biopolymers*, 17 (1978) 2663–2678.
17 E. R. MORRIS, D. A. REES, G. YOUNG, M. C. WALKINSHAW, AND A. DARKE, *J. Mol. Biol.*, 110 (1970) 1–16.
18 E. R. MORRIS, in P. A. SANDFORD AND A. LASKIN (Eds.), *Extracellular Microbial Polysaccharides, ACS Symp. Ser.*, 45 (1977) 81–89.
19 G. PARADOSSI AND D. A. BRANT, *Macromolecules*, 15 (1982) 874–879.
20 E. R. MORRIS, *Food Chem.*, 6 (1980) 15–39.
21 M. MILAS AND M. RINAUDO, in D. A. BRANT (Ed.), *Solution Properties of Polysaccharides, ACS Symp. Ser.*, 150 (1981) 25–30.
22 G. MARET, M. MILAS, AND M. RINAUDO, *Polym. Bull.*, 4 (1981) 291–297.
23 V. J. MORRIS, K. I'ANSON, AND C. TURNER, *Int. J. Biol. Macromolecules*, 4 (1982) 362–366.
24 J. G. SOUTHWICK, H. LEE, A. M. JAMIESON, AND J. BLACKWELL, *Carbohydr. Res.*, 84 (1980) 287 297.
25 J. G. SOUTHWICK, M. E. MCDONNELL, A. M. JAMIESON, AND J. BLACKWELL, *Macromolecules*, 12 (1979) 305–311.
26 S. A. FRANGOU, E. R. MORRIS, D. A. REES, R. K. RICHARDSON, AND S. B. ROSS-MURPHY, *J. Polym. Sci., Polym. Lett. Ed.*, 20 (1982) 531–538.
27 R. W. WHORLOW, *Rheological Techniques*, Wiley, London, 1980, pp. 115–187.
28 B. J. BERNE AND R. PECORA, *Dynamic Light Scattering*, Wiley, London, 1976.
29 H. UTIYAMA, in M. B. HUGLIN (Ed.), *Light Scattering from Polymer Solutions*, Academic Press, New York, 1972, pp. 41–60.
30 J. CABANNES AND Y. ROCHARD, *La diffusion moléculaire de la lumière*, University of France Press, Paris, 1929.
31 C. TANFORD, *Physical Chemistry of Macromolecules*, Wiley, London, 1961, pp. 275–314.
32 B. CHU, *Laser Light Scattering*, Academic Press, New York, 1974, pp. 208–209.
33 E. FREDERICQ AND C. HOUSSIER, *Electric Dichroism and Electric Birefringence*, Clarendon Press, Oxford, 1973.
34 J. G. SOUTHWICK, A. M. JAMIESON, AND J. BLACKWELL, in D. A. BRANT (Ed.), *Solution Properties of Polysaccharides, ACS Symp. Ser.*, 150 (1981) 1–13.
35 J. G. SOUTHWICK, A. M. JAMIESON, AND J. BLACKWELL, *Carbohydr. Res.*, 99 (1982) 117–127.
36 J. G. SOUTHWICK, Ph.D. Thesis, Case Western Reserve University, 1981.
37 V. J. MORRIS, G. J. BROWNSEY, AND B. R. JENNINGS, *Mol. Phys.*, 37 (1979) 303–315.
38 V. CARROLL, G. R. CHILVERS, D. FRANKLIN, M.J. MILES, V. J. MORRIS, AND S. G. RING, *Carbohydr. Res.*, 114 (1983) 181–191.
39 V. N. TSVETKOV, E. I. RJAMTSEV, AND I. N. SHTENNIKOVA, in A. BLUMSTEIN (Ed.), *Liquid Crystalline Order in Polymers*, Academic Press, New York, 1978, pp. 43–103.
40 P. J. HAGERMAN AND B. ZIMM, *Biopolymers*, 20 (1981) 1481–1502.
41 G. M. HOLZWARTH, *Carbohydr. Res.*, 66 (1978) 173–186.
42 V. J. MORRIS, A. R. FOWERAKER, AND B. R. JENNINGS, *Adv. Mol. Relaxation Interaction Processes*, 12 (1978) 65–83.
43 J. M. BURGERS, *Verh. K. Ned. Akad. Wet. Afd. Natuurkd.*, 16 (1938) 113.
44 N. A. J. HASTINGS AND J. B. PEACOCK, *Statistical Distributions*, Butterworths, London, 1975.
45 E. F. PASCHALL, U.S. Pat. 2,935,509, May 1960.